

---

# Effect of Heating and Resistance on Emission Properties of Carbon Nanotubes

Sergey V. Bulyarskiy<sup>1\*</sup>, Alexander A. Dudin<sup>1</sup>, Alexander V. Lakalin<sup>1</sup>, Andrey P. Orlov<sup>1</sup>, Alexander A. Pavlov<sup>1</sup>, Roman M. Ryazanov<sup>2</sup>, Artemiy A. Shamanaev<sup>2</sup>

<sup>1</sup> Institute of Nanotechnology of Microelectronics of the Russian Academy of Sciences, 32A Leninskii pr., Moscow, 119991, Russia, E-mail: bulyar2954@mail.ru

<sup>2</sup> Scientific-Manufacturing Complex «Technological Centre» build 1, Shokin sq., Zelenograd, Moscow, 124498, Russia

---

## ABSTRACT

We have studied the effect of the series resistance on the heating of the cathode, which is based on carbon nanotubes and serves to realize the field emission of electrons into the vacuum. The experiment was performed with the single multi-walled carbon nanotube (MCNT) that was separated from the array grown by CVD method with thin-film Ni-Ti catalyst (nickel 4 nm / Ti 10 nm). The heating of the cathode leads to the appearance of a current of the thermionic emission. The experimental voltage current characteristic exhibited the negative resistance region caused by thermal field emission. This current increases strongly with increasing voltage and contributes to the degradation of the cold emitter. The calculation of the temperature of the end of the cathode is made taking into account the effect of the phenomenon that warms up and cools the cathode. We have developed a method for processing of the emission volt-ampere characteristics of a cathode, which relies on a numerical calculation of the field emission current and the comparison of these calculations with experiments. The model of the volt-ampere characteristic takes into account the CNT's geometry, properties, its contact with the catalyst; heating and simultaneous implementation of the thermionic and field emission. The calculation made it possible to determine a number of important parameters, among which the voltage and current of the beginning of thermionic emission, the temperature distribution along the cathode, the resistance of the nanotube. The phenomenon of thermionic emission from CNT's was investigated experimentally and theoretically. The conditions of this type emission occurrence were defined. The results of the study could form the basis of theory of CNT emitter's degradation.

**Keywords:** Carbon Nanotubes; Field Emission; Thermionic Emission; Volt-ampere Characteristic; Emitter Temperature

---

## 1. Introduction

The carbon nanotubes (CNT's) have the important practical properties such as high electrical and thermal conductivity, suitable mechanical properties, ability to absorb and emit electromagnetic waves<sup>[1]</sup>. Scientists from all over the world have developed the variety of convenient technological methods for producing CNT's, which promotes the development of studies of this allotropic form of carbon. At present, various practical applications of nanotubes are shown, including field-effect transistors, lithium-ion batteries, radiation receivers, interconnections of integrated microcircuits, conductive composites, etc.<sup>[1]</sup>. CNT's have a small diameter. For the case with single-walled CNT, it is from 0.8 to 1.5 nm, for multi-walled CNT - from units to tens nanometers. CNT's diameter is much less than

their length (large aspect ratio), it results in enhancement of the electric field near the CNT's tip and contributes to field emission. Several papers that appeared in 1995 described the phenomenon of field emission in CNT's<sup>[2-4]</sup>. This phenomenon formed the basis for a number of important applications from the point of view of practical applications: flat screens<sup>[5,6]</sup>, miniature X-ray tubes<sup>[7,8]</sup>, light-emitting devices<sup>[9,10]</sup>, miniature vacuum lamps<sup>[11,12]</sup>, terahertz amplifiers<sup>[13,14]</sup>, high-frequency vacuum switches<sup>[15]</sup>.

For widespread use of field emission (FE) it is necessary to study the possibility of achieving high emission current densities and stability of this process. These issues are discussed in detail foremost from the theoretical point of view, in particular, the necessary information can be found in the reviews<sup>[16,17]</sup>.

Voltage-current characteristic of cold cathode in the region of prevalence of field emission current is generally described by Fowler-Nordheim formula. Detailed analysis of this model and its transition to the region of thermionic emission was carried out in<sup>[15,18]</sup>. The calculations of field-emission current for CNT were shown in several studies, for example, in<sup>[15-19]</sup>. Fowler-Nordheim dependence in usable form has a form<sup>[20]</sup>:

$$J = \frac{e^3 E^2}{8\pi h \phi t^2(y)} \exp\left(-\frac{8\pi\sqrt{2m}\phi^{3/2}\theta(y)}{3heE}\right), \quad (1)$$

where:  $t(y) = 1 + 0.1107 \cdot y^{1.33}$ ,  $\theta(y) = 1 - y^{1.69}$ ,  $y = \frac{e}{\phi} \sqrt{\frac{eE}{4\pi\epsilon_0}}$ ,  $e$  is elementary charge (C),  $h$  is Plank constant (J·s),  $E$  is the local electric field strength near the emitting surface (V/m),  $\phi$  is work function of an electron from a CNT (J),  $m$  is free-electron mass,  $J$  is current density of the FE (A/m<sup>2</sup>).  $t(y_0)$  и  $v(y_0)$  are weakly varying functions that can be taken equal to unity without increasing the error in determining the work function. We can neglect the weak power dependence of the functions  $t(y)$  and  $\theta(y)$  by setting  $t(y) \approx 1$  and  $\theta(y) \approx 1$ . This condition allows us to obtain the following formula for calculating of the work function:

$$J = 1.54 \cdot 10^{-6} \frac{E^2}{\phi} \exp\left(-\frac{6.83 \cdot 10^9 \phi^{3/2}}{E}\right), \quad (2)$$

where:  $[\phi]=\text{eV}$ ,  $[E]=\text{V/m}$ ,  $[J]=\text{A/m}^2$ .

The experimental results are often represented in the Fowler-Nordheim coordinates:  $\ln(J/E^2) = f(1/E)$ . A straight line approximates these results and the work function is calculated from the slope of which. The amount of the calculation these work function depends on the choice of the initial and final electric field strengths, which specify the region of the current-voltage characteristic. In generally, this choice is not motivated. Therefore, the result of calculating contains significant systematic errors.

Even in the first papers devoted to field emission, it was found that CNT's tip is heated by flow of field-emission current, and its temperature is proportional to the square of the current density<sup>[19,21]</sup>, which is quite obvious in accordance with the Joule-Lenz law. Models that are more complex were considered in<sup>[16,17]</sup>.

A single nanotube has a rather large thermal resistance. This resistance prevents the release of heat into the substrate with which the lower end of the nanotube is connected. CNT's tip heating leads to thermionic emission current, which may be large and even exceed the field emission current. Moreover, the resistance of CNT's changes the voltage-current characteristic as a function of temperature and current value due to an additional voltage drop. CNT's resistance makes a definite contribution to the form of the voltage-current characteristic, taking part of the voltage to itself at high current densities. Thus, CNT's resistance leads to a deviation of the experimental results from Ed. (1). Therefore, when researchers involve only Fowler-Nordheim dependence to determine the work function, they admit two systematic errors: firstly, thermionic emission is neglected, and, secondly, they don't taking into account the voltage drop on the nanotube.

In this paper, the emission currents of a single multi-walled nanotube have been studied experimentally in a wide range of current values. The authors have revealed deviations of the current-voltage characteristic from the Fowler-Nordheim dependence. Moreover, the calculation of the temperature of CNT's heating has been carried out, the conditions under which the nanotube resistance and the thermionic emission current have a significant effect to the voltage-current characteristic shape were analyzed, and the algorithm for CNT parameters calculating was presented, namely: the electrical resistance, the dependence of the CNT heating temperature from the current value.

## 2. Experimental results

Carbon nanotubes were grown by the chemical vapor deposition (CVD) method in «Plasmalab System 100» (Oxford Instruments) on silicon substrate on which a catalyst was deposited consisting of a two-layer metal film: titanium 10 nm and nickel 2 nm. The film of the catalyst was covered with silicon oxide, in which windows were opened with a diameter of 0.7  $\mu\text{m}$ . The CNT growth was carried out by CVD method. Gas flow consisted from an acetylene with addition of ammonia in a 3:1 ratio rate. It was constant during the growth process. The synthesis temperature was 600 ° C. As a result, single multi-walled carbon nanotubes 2-3  $\mu\text{m}$  in height were obtained (**Figure 1**).

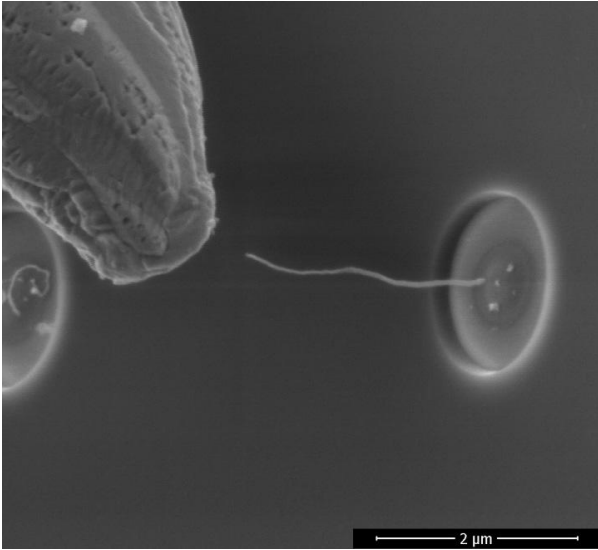


**Figure 1;** SEM image of single multi-walled carbon nanotube (cathode) and tungsten tip (anode).

The measurements were carried out in a high vacuum in the chamber of two-beam FEI Helios NanoLab 650i system. A measuring electron microscope could obtain images with a resolution of not worse than 0.7 nm at an accelerating voltage of not more than 1 kV. The pressure in the measuring chamber was  $5 \cdot 10^{-5}$  Pa. In this chamber there was a probe system Kleindiek Nanotechnik with 4 separate independent manipulators that can operate at voltages up to 150 V. Each probe had its own coaxial connector. For current-voltage measurements on DC currents, a programmable two-channel source-meter Source Meter 2634B from Keithley was used. This device can measure currents up to  $10^{-15}$  A. It is equipped with special shielded three axial leads with the function of ultra-low currents compensation. The input impedance of source-meter (over 100 Volts) provides a minimum level of the introduced distortions and errors in tested circuits during the measurements for this class of instruments.

The voltage-current characteristic of emission current of the single multi-walled CNT is shown in **Figure 2**. It was the starting point for further processing. The electrical circuit in which the emission current flows is shown in the inset to **Figure 2**. This current consists of two components: its nonlinear resistance characterizes field emission and thermionic emission, each of these processes ( $R_{FE}$  and  $R_{TE}$ ). The total voltage applied to the circuit ( $U$ ) is composed of the sum of the voltages, one of which falls on the resistance of the nanotube ( $U_R$ ), and the other one - on the nonlinear resistance of the emitting tip of the nanotube ( $U_E$ ). We must divide the current of the current-voltage characteristic into two components. One component is the field emission

current, and the second component is the thermionic current. These components are determined by the following sequence of actions:

1) The field emission current is calculated (the calculations are shown in the following subsection). The work function is selected in such way that the field-emission current coincides with the initial section of the experimental voltage-current characteristic (**Figure 2**). This calculation allows us to determine  $U_F$ .

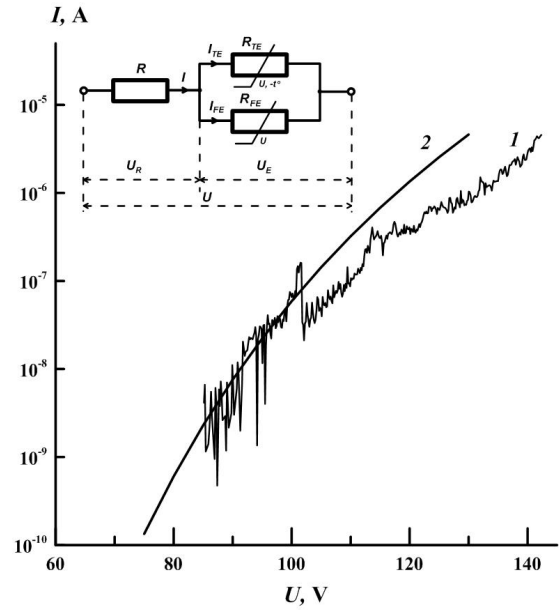


**Figure 2;** Voltage-current characteristic of the emission current of the single multi-walled CNT: 1 - experimental, 2 - modeling by formula (3). Top corner: equivalent circuit of CNT.

2) The voltage of the model curve there is a deduction from the voltage of the experimental curve for each current value. The difference of these voltages makes it possible to determine  $U_R$  (**Figure 2**), to construct the current-voltage characteristic of the series resistance of a carbon nanotube and calculate this resistance  $R=10$  M $\Omega$ . Then the model value of the voltage drop across the series resistance of a nanotube is:  $U_R = I \cdot R$ .

3) We are conducting the second stage of modeling the volt-ampere characteristic. The total theoretical voltage ( $U_t$ ), which should be on the emission system, is calculated as the sum of the voltage on the nonlinear resistance of the emitting tip of the nanotube ( $U_E$ ) and the series resistance ( $U_R$ ). We calculate the difference between the theoretical and experimental voltage drops at each current value:  $U_t - U = U_E + U_R - U$ . The result is a voltage-current characteristic of the section, which contains two parallel non-linear resistances ( $R_{FE}$  and  $R_{TE}$ ). The result of the transformations is shown in

**Figure 3.** This figure shows the initial experimental current Ed.(1); field emission current Ed. (2); the experimental section of negative resistance Ed. (3). The voltage reaches a critical value ( $U_c$ ) at a critical value of the current ( $I_c$ ). Further increases of the current leads to a heating of the nanotube, as a result of which, the resistance for the thermionic current decreases. This leads to a decrease in voltage drop across the parallel connection section of nonlinear resistances. The voltage at the end of the nanotube, which emits electrons, falls and the emission current decreases. It is evident that when CNT's tip is heated to a certain critical temperature, a thermionic emission current appears, and the voltage at the emitting end ( $U_E$ ) is falls. A section of negative resistance is present, then:  $I > I_c$ . The current that exceeds the critical region is thermionic in fact. The field emission current does not exceed the critical current.

Thus, the thermionic current component dominates when the total current density exceeds a critical value. This is because the end of the tube is heating when the current flows. The temperature of the end of the tube grows. Its temperature can reach several thousand degrees. This temperature leads to CNT destruction and the emission current degrades. The phenomenon of degradation of the field emission current is due to overheating of the nanotube. Below, we will carry out the necessary calculations to determine the conditions under which the emission process will be stable.

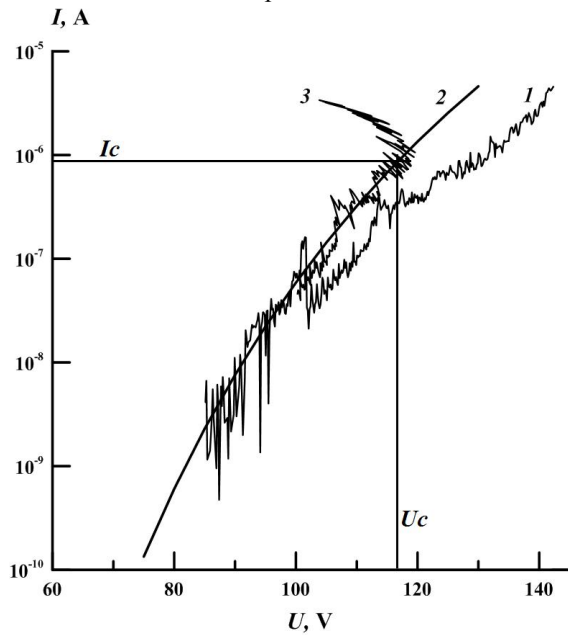


**Figure 3;** Current-Voltage characteristics of the investigated CNT: 1 - experimental I-V characteristic, 2 - modeling I-V characteristic (Ed. 3), 3 - I-V characteristic of the section, which contains two parallel non-linear resistances ( $R_{FE}$  and  $R_{TE}$ ).

### 3. Modelling

#### 3.1 Calculation of the currents of the field emission of a carbon nanotube (CNT)

The efficiency of field emission depends essentially on the electric field strength near the emitting surface. Therefore, the electric field strength requires an exact calculation. The calculation is carried out in two stages: first, the potential distribution and the magnitude of the electric field at the end of the tube are calculated; secondly, the current density of the cathode is calculated. The calculation of the electric field potential distribution is carried out in the classical approximation. We applied a model in which a CNT is a solid body of cylindrical shape. The end of this body represents a hemisphere (CNT with a closed end) or half a torus (CNT with an open end). This body has a metallic type of conductivity. The potential of the electric field is found by solving the 3-dimensional Laplace equation in the boundary element with the conditions given on it's boundary. The solution of the Laplace equation was found by the boundary element method, which is described in detail in<sup>[22,23]</sup>. This method involves splitting the surface of a solid body into triangular elements and forming the computational grid. Then the boundary conditions are given on its boundaries. As a result, instead of solving the integral equation, a system of linear algebraic equations is solved. By solving, we obtain the coefficients required for calculating the potentials in corresponding space points of emission system.

Partitioning of the boundary surface to boundary elements (BE), on the one hand, need to be quiet detailed to consider all special aspects of surface and on the other hand should not exceed a certain value due to the computing power used by the computer (memory capacity, processing speed). Based on these conditions, in this case, the entire boundary surface is divided into 20000 - 30000 triangular BE.

Electric field strength distribution must be calculated near all points of the CNT surface, since the cathode current is caused not only by emission from its end, but also from regions near it. **Figure 4** shows the emission system under investigation consisting of a single CNT (cathode) and an anode electrode, as well as its idealized model, which was later used to calculate the

distribution of the electric field and the field emission current.

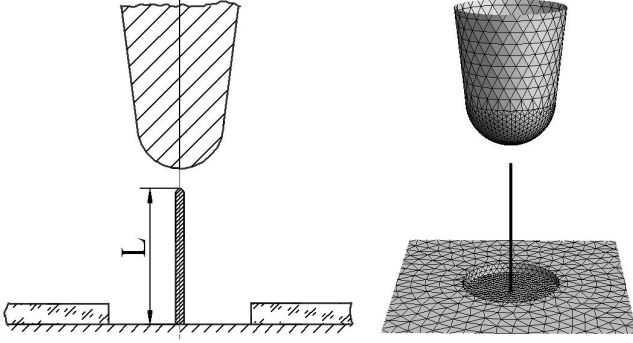


**Figure 4;** Model of a single CNT (cathode) and an anode electrode.

Geometric parameters of the calculation were obtained as a result of determining the size of a real experimental system, which is shown in **Figure 1**.

A system of equipotential surfaces was obtained after the implementation of the above mentioned calculation algorithm. The electric field strength was calculated as the potential gradient near the surface.

The cathode current is the sum of the current of the total boundary elements. Electrons, which are emitted by these elements, moved along a certain trajectory and, at the end of their path, hit the anode. The motion of an electron along a trajectory causes the formation of an elementary electric current. The sum of these currents over the area of the cathode creates an emission current (cathode current), as well as the components of this current that fall on other elements of the emission system (anode current, leakage current, etc.). Such approach is permissible on the basis of an estimate of the electron velocity in the system. The velocity of an electron in the corresponding electric field can be estimated from the law of energy conservation:

$$V = c \sqrt{1 - \left( \frac{m_0 c^2}{m_0 c^2 + eU} \right)^2},$$

Where:  $c$  is light velocity;  $m_0$  is electron rest mass;  $U$  is accelerating voltage between cathode and anode. In the experiments  $U$  did not exceed 150 V, therefore  $V \leq 5 \cdot 10^6$  m/s.

Thus, the electron velocity is much smaller than the speed of light, so they move with nonrelativistic velocities and the laws of classical mechanics can be used to calculate their trajectories of motion. We will assume that the Coulomb force acts on the electron, which must be used in the motion equation. The numerical integration was done by Euler's method<sup>[24]</sup>. It

should be noted that in the case of random cathode geometry (not flat) in Eqs. (1) and (2)  $E$  is understood as the field strength near the surface of the emitting elementary cathode pad, rather than the average value obtained by dividing the applied voltage by the distance between the anode and the cathode. When calculating the field-emission current from a single CNT, it is assumed that each BE of the cathode emits a current  $I_i$ , which is defined as  $I_i = J_i \Delta S_i$  where  $J_i$  is the current density of the  $i$ -th BE of cathode,  $\Delta S_i$  is the surface area of the  $i$ -th cathode BE (the surface area of the entire cathode  $S = \sum_i \Delta S_i$ ). The current density  $J_i$  is calculated from the

Fowler-Nordheim Eq. (1), in which the electric field strength  $E_i$  is taken from the solution of the Laplace equation for a given initial point at the center of each  $i$ -th BE. Then the total field emission current of the cathode is found by summing the currents over all sites  $\Delta S_i$ :

$$I = \sum_i J_i \Delta S_i = \sum_i \frac{e^3 E_i^2}{8\pi h \phi i^2(y_i)} \exp\left(-\frac{8\pi\sqrt{2m}\phi^{3/2}\theta(y_i)}{3heE_i}\right) \Delta S_i. \quad (3)$$

### 3.2 Calculation of the heating temperature of the end of a single carbon nanotube

The nanotube is heated when an electric current flows in it. Its temperature is not the same at its two ends. It is assumed that the temperature of the nanotube end, which is in contact with the substrate, is equal to the temperature of the substrate. The temperature of the opposite end was calculated by solving the heat-transfer equation taking into account the radiative cooling and the release of heat, which is caused by the current flow<sup>[21,25]</sup>:

$$S \frac{d}{dx} \left( k(T) \frac{dT}{dx} \right) dx - 2\pi r \eta \sigma (T^4 - T_0^4) dx + I^2 \frac{R(T)}{L} dx = 0, \quad (4)$$

Where:  $S = \pi(r^2 - r_0^2)$  is cross-section area of CNT,  $r$  is outer radius of CNT,  $r_0$  is inner radius of CNT,  $k(T)$  is coefficient of heat conductivity along the CNT axis,  $T = T(x)$  is the temperature along the CNT axis,  $T_0$  is the temperature of surrounding bodies (substrate),  $L$  is length of CNT,  $R(T)/L$  is electrical resistance of a unit length of CNT,  $\eta$  is the coefficient of the grayness of the thermal radiation of CNT ( $\eta < 1$ ) in our case was taken equal to 0.9,  $\sigma = 5.67 \cdot 10^{-8} \text{ W}/(\text{m}^2 \text{K}^4)$  is Stefan-Boltzmann constant,  $I$  is the current, flowing through CNT (emission current). The boundary conditions for equation (4) have the form:

$$T(0) = T_0, \quad \frac{dT(L)}{dx} = 0. \quad (5)$$

In Ref.<sup>[21]</sup> the analytical solution of Eq. (4) was obtained in the absence of radiative cooling and provided that the thermal conductivity coefficient  $k$ , as well as the resistance  $R$  of the nanotube, do not depend on temperature. However, for the case with CNTs there is a temperature dependence of  $k$  and  $R$ , therefore the results of<sup>[21]</sup> should be considered as approximate. It was assumed in<sup>[25]</sup> that the thermal conductivity coefficient  $k$  and the resistance  $R$  are described by power functions of temperature. For the case:  $k = aT^3$ ,  $R = bT^4 + c$  in<sup>[25]</sup> an analytic solution of Ed. (4) was obtained. In Ref.<sup>[26]</sup> it was assumed that:  $k = k_0(T/T_0)^\alpha$ ,  $R = R_0(T/T_0)^\alpha$ , where  $\alpha$  is an adjustable parameter, and equation (4) was solved numerically.

However, power-law dependence with the form  $k = CT^\alpha$  for the thermal conductivity coefficient occurs only at temperatures below the Debye characteristic temperature<sup>[27]</sup>. At high temperatures, due to the anharmonicity of long-wave oscillations and other causes, the thermal conductivity of a solid body decreases according to the law  $1/T$ , namely<sup>[27]</sup>

$$k = k_0 \frac{\Theta}{T}, \quad (6)$$

where:  $\Theta$  is Debye temperature. The energy of the Debye phonon of carbon nanotubes is 0.103 eV [28]. Accordingly, the Debye temperature is  $\Theta=1190\text{K}$ . It is the dependence that dominates in the high-temperature

$$\begin{cases} k_0 \frac{\Theta}{T} S \left( \frac{d^2 T}{dx^2} - \frac{1}{T} \left( \frac{dT}{dx} \right)^2 \right) - 2\pi r \eta \sigma (T^4 - T_0^4) + I^2 \frac{\rho_0 (1 - \alpha T + \beta T^{3/2})}{S} = 0; \\ T(0) = T_0; \\ \frac{dT(L)}{dx} = - \frac{\sigma}{k_0 \frac{\Theta}{T(L)}} (T^4(L) - T_0^4) - \frac{3k_B T(L)}{2} \cdot \frac{I}{ek_0 \frac{\Theta}{T(L)} S}; \end{cases} \quad (8)$$

The system that is given by Ed. (8) is solved by a numerical method to determine the temperature of the end of a nanotube that emits electrons. The values of the parameters were assumed to be equal to:  $\alpha=8.5 \cdot 10^{-4} \text{K}^{-1}$ <sup>[31]</sup>,  $\beta=9.8 \cdot 10^{-6} \text{K}^{-3/2}$ <sup>[31]</sup>,  $\rho_0=2.33 \cdot 10^{-3} \Omega \cdot \text{m}$ <sup>[31]</sup>,  $L=2.36 \mu\text{m}$ ,  $r=20 \text{ nm}$ ,  $r_0=15 \text{ nm}$ ,  $T_0=300 \text{ K}$ ,  $I=10 \text{ uA}$ ,  $\Theta=1190 \text{ K}$ ,  $k_0=140 \text{ W}/(\text{m} \cdot \text{K})$ . At the selected values of  $k_0$  and  $\Theta$  in

region, when thermionic emission is possible. Therefore, for calculating the heating of the nanotube, the dependence Ed.(6) was chosen.

The correct calculation of the temperature of nanotubes should be taken into account both their heating due to Joule heat, and cooling due to the Nottingham effect<sup>[29]</sup>. The Nottingham effect is manifested in the cooling of the cathode. This effect is the result of the difference between the average energy of the electrons that leave the cathode and the electrons from the volume of the nanotube that takes their place. The electron that leaves the CNT carries away from the nanotube energy equal to the average energy of the thermal motion  $(3/2)k_B T$  <sup>[30]</sup>. The number of electrons that are emitted from the cathode per unit time is  $I/e$ . Then the boundary condition Ed. (5) at the point  $x=L$  will have the form:

$$\frac{dT(L)}{dx} = - \frac{\sigma}{k} (T^4(L) - T_0^4) - \frac{3k_B T(L)}{2} \cdot \frac{I}{ekS}.$$

The first term describes the cooling of CNTs by radiation from the end surface<sup>[29,30]</sup>, the second term due to the Nottingham effect<sup>[30]</sup>. In addition, the temperature dependence of the resistance of CNTs has the form<sup>[30,31]</sup>:

$$R(T) = \frac{L}{S} \rho_0 (1 - \alpha T + \beta T^{3/2}), \quad (7)$$

Where:  $\rho_0$  is the resistivity of an CNTs.

The heat conduction Ed. (4) takes the form with allowance for Ed (6), (7):

the temperature range 200-1000 K, the thermal conductivity coefficient  $k$  lies in the range  $55 \div 830 \text{ W}/(\text{m} \cdot \text{K})$ . This corresponds to the literature data according to which  $k$  can vary from 25 to 3000  $\text{W}/(\text{m} \cdot \text{K})$ <sup>[25]</sup>. The results of the calculations are shown in **Figure 5**, curve 1 (curve 2 - calculation without taking into account the Nottingham effect).



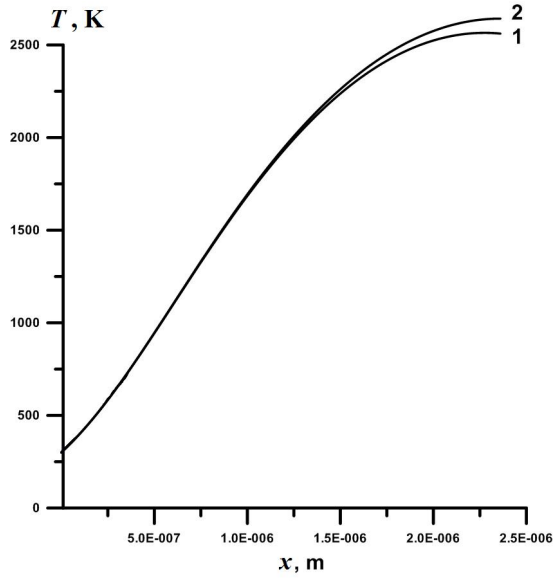


**Figure 5;** Temperature distribution along the axis of the carbon nanotube: 1 - taking into account (1) the Nottingham effect, 2 - without taking into account the Nottingham effect. The values of the coefficients are indicated in the text.

**Figure 6** shows the temperature dependence of the emitting end of the CNT's ( $T_L$ ) as a function of the flowing emission current, taking into account the Nottingham effect (for comparison, the curve for  $k=\text{const}$  is also given there). The calculation is made for the values of the coefficients, which are given in the text before that. The temperature of the emitting end of the CNT in the case  $k=k_0(\Theta/T)$  turned out to be higher than in the case  $k=\text{const}$  in the whole considered range of emission currents.

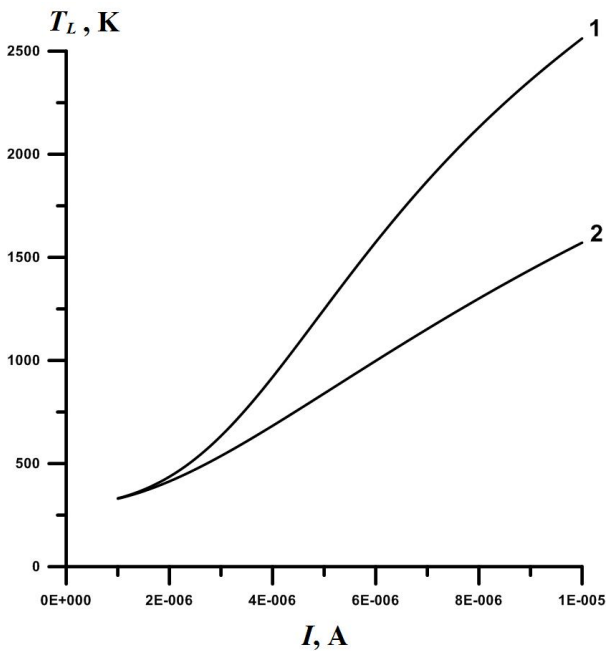


**Figure 6;** The temperature of the emitting end of CNTs on the value of the flowing emission current, taking into account

the Nottingham effect. 1 -  $k=k_0(\Theta/T)$ ; 2 -  $k=\text{const}$ . The values of the coefficients are shown in the text.

The nanotube length varied from 0.5 to 4  $\mu\text{m}$  when calculating the temperature. The temperature of the cold end of the nanotube contacted to the substrate was assumed to be  $T_0 = 300\text{ K}$ .

Equation (4) was solved for different values of the current  $I$ , and thus a dependence  $T_L - T_0 = f(I)$  was obtained, where  $T_L$  is the temperature of the emitting end,

**Figure 7.**

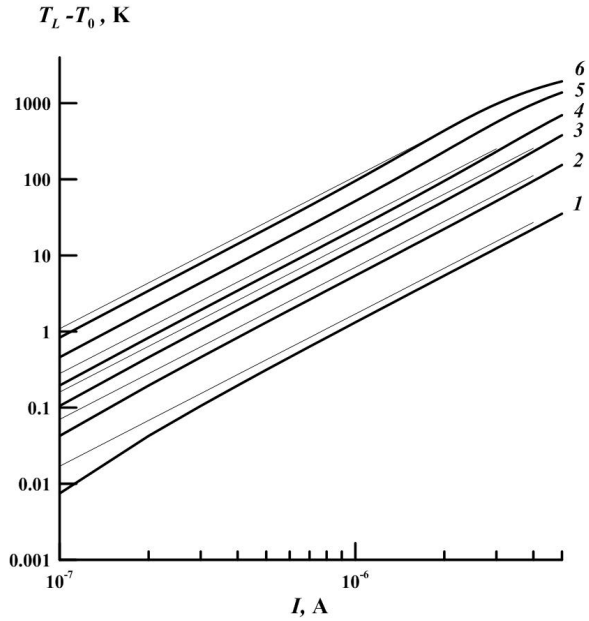


**Figure 7;** Dependence of the superheating temperature of the emitting end of a CNT on the flowing current for CNTs of different lengths: 1 - 0.5  $\mu\text{m}$ , 2 - 1.0  $\mu\text{m}$ , 3 - 1.5  $\mu\text{m}$ , 4 - 2.0  $\mu\text{m}$ , 5 - 3.0  $\mu\text{m}$ , 6 - 4.0  $\mu\text{m}$ .

In this figure, the exact solution of Ed. (4) is compared with the approximate analytical solution obtained under the condition that there are no radiative cooling, no Nottingham effect, the thermal conductivity coefficient and the resistance of CNTs are constant<sup>[21]</sup>:

$$T_L - T_0 = \frac{I^2 R}{2kS} L \quad (9)$$

The results of the calculations in **Figure 7** show that the simplified solution gives an overestimate value of the superheat temperature of the emitting end of the nanotube for all values of its length. A simplified solution approximates the exact solution with increasing current strength. We assume that the temperature dependence of the thermal conductivity Ed. (6) is compensated by additional cooling due to the Nottingham effect. The temperature of the cathode overheating increases in proportion to the square of the

emission current. The current strength of the 1 uA is a critical value in our case, exceeding which results in the appearance of thermionic emission currents and the appearance of unstable volt-ampere characteristics.

#### 4. Results and discussion

The emission current is composed of the field and thermionic components according to the electrical circuit of the current flow is shown in **Figure 2**. This current is represented by curve 3 in **Figure 3**. Field emission current is represented by curve 2. It is obvious that at the maximum values of the voltage ( $U_c$ ) at which the negative resistance region starts, the currents of field-electron and thermionic emission are approximately equal. Further current growth is due to the thermionic component, and the field current decreases, while changing along curve 2.

Thus, the region of negative resistance of the voltage-current characteristic (**Figure 3**) is due to the fact that the current of thermionic emission predominates over the field emission current. The end of the nanotube is already overheated to such an extent that it can be destroyed. The voltage ( $U_c$ ) and current ( $I_c$ ) at which the negative resistance region starts can be considered as critical. As soon as the total current exceeds this value, the emission becomes unstable and the degradation processes begin.

It is important to estimate the conditions under which degradation of emission currents is possible. There is a conditional current limit, the excess of which causes a rapid overheating of the nanotube end and the degradation of the emission. At the boundary, the total current is equal to the sum of the currents of the field electron emission and the thermionic emission,  $I = I_{TE} + I_{FE}$ .

Subsequently thermionic current predominates. Therefore, as a condition for changing the emission mechanism, one can choose the equality of currents  $I_{TE} = I_{FE}$  or  $I_{TE}(T) = I/2$ . This condition allows us to estimate the geometric dimensions of the carbon nanotubes of the cathode at a fixed value of the flowing current at which their heating begins.

The temperature of CNT end warming up is determined by the current of thermionic emission ( $I_{TE}$ ) and the geometric dimensions of the nanotube, which ultimately determine the magnitude of its electrical resistance Ed. (9). For rough estimation of the overheating temperature it is enough to restrict ourselves to Ed. (9). The resistance of a nanotube is estimated by the formulas

$$R = \rho \frac{L}{S}, \quad \rho = R_0 \frac{S_0}{L_0}, \quad (10)$$

where: - CNT  $S = \pi(r^2 - r_0^2)$  cross-section area. The values of these parameters were calculated from the experiments  $R_0=10 \text{ M}\Omega$ ,  $S_0=5.5 \cdot 10^2 \text{ nm}^2$ ,  $L_0=2.36 \text{ }\mu\text{m}$ ,  $\rho=2.33 \cdot 10^{-3} \text{ }\Omega \cdot \text{m}$ . The expression for the thermionic emission current is:

$$I_{TE} = S_{CNT} \frac{4\pi m_n^*}{h^3} (kT)^2 \exp \left[ -\frac{\varphi - \sqrt{e^3 E / (4\pi\epsilon_0)}}{k_B T} \right], \quad (11)$$

where:  $S_{CNT} = 2\pi r^2$  is the area of CNT emitting surface (hemisphere surface area),  $m_n^* = 0.3m$  is effective mass of electron in CNT,  $k_B$  is Boltzmann constant,  $T$  is absolute temperature,  $\epsilon_0$  is electrical constant.

The conditional boundary of the transformation of a stable process to an unstable process is calculated from formulas (10) and (11). If we neglect the decrease in the height of the barrier in the formula (11) by the electric field, then the condition  $I_{TE}(T) = I/2$  will be written in the form:

$$\frac{1}{2} I = S_{CNT} A (T(L))^2 \exp \left[ -\frac{\varphi}{k_B T(L)} \right]. \quad (12)$$

Substituting Ed. (9) into Ed. (12), we obtain:

$$\frac{I}{S_{CNT}} = 2A \left( T_0 + \frac{I^2 \rho L^2}{2kS^2} \right)^2 \exp \left[ -\frac{\varphi}{k_B \left( T_0 + \frac{I^2 \rho L^2}{2kS^2} \right)} \right]. \quad (13)$$

For the case with given CNT radius  $r$ , formula (13) allows us to calculate the cross-sectional area  $S$  and the length  $L$ , which correspond to the beginning of the appearance of the thermionic emission current ( $I_{TE}$ ) for a given value of the total current  $I$ , **Figure 8**.



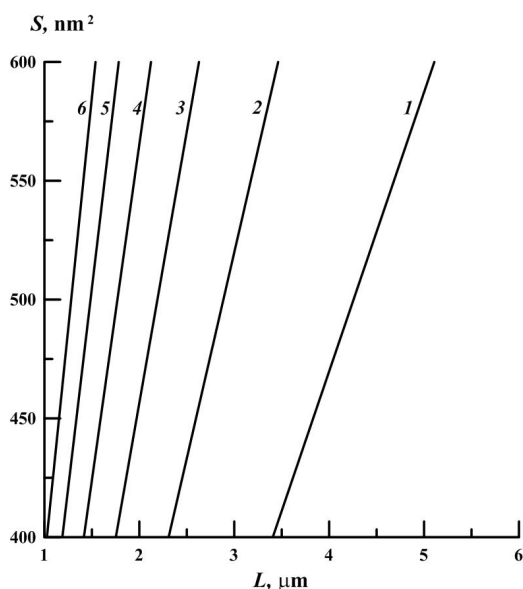


**Figure 8;** Dependencies for current values  $I$ : 1 - 2  $\mu\text{A}$ , 2 - 3  $\mu\text{A}$ , 3 - 4  $\mu\text{A}$ , 4 - 5  $\mu\text{A}$ , 5 - 6  $\mu\text{A}$ , 6 - 7  $\mu\text{A}$ .

This figure represents several regions in the space of length - CNT area. This space is divided into regions by the curves, which are calculated for certain currents. These curves represent the boundary behind which the regime of thermionic emission and degradation of CNTs occurs. For each curve, the following statement is true: if the length of the nanotube is larger and the area is smaller, then we cross the boundary and fall into the degradation region.

With inverse relations between the parameters, namely: the length is less than the boundary one, and the area is larger, we fall into the region of stability of the emission.

## 5. Summary and conclusions

The analysis of emission processes with a single nanotube showed that when the current density increases, the end that emits electrons is heated. In this case, along with the field emission current, a thermionic emission current appears. The growth of the total current causes overheating of the end of the nanotube. This current is almost completely associated with the phenomenon of thermionic emission. At the same time, the emission process becomes unstable. So the temperature of overheating can exceed 1000 °C, and then the nanotube begins to break down.

To analyze these processes, within the framework of this work an algorithm has been developed that relies on numerical calculations of the field emission current and the overheat temperature. It is shown that when there is overheating, a negative resistance region occurs. At this moment, the thermionic current begins to

predominate. The correlation between the current density, length and cross-sectional area of the nanotube was calculated, which allows estimating the regions in which cathode degradation can progress and the emission becomes unstable.

## Acknowledgments

The work was carried out with the financial support of the Ministry of Education and Science of Russia (project No. 16.9007.2017 / БЧ).

## References

1. Bulyarskiy S.V. Carbon nanotubes: Technology. Manage properties. Application. Ulyanovsk: Strezhen; 2011. 479 p. [in Russian].
2. Chernozatonskii L.A., Gulyaev Y.V., Kosakovskaja Z.J., Sinityn N.I., Torgashov G.V., Zakharchenko Yu.F., Fedorov E.A., Val'chuk V.P. Electron field emission from nanofilament carbon films. Chem. Phys. Lett. 1995; 233: 63-68.
3. De Heer W.A., Chatelain A., Ugarte D. A carbon nanotube field-emission electron source. Science 1995; 270: 1179-1180.
4. Rinzler A.G., Hafner J.H., Nikolaev P., Nordlander P., Colbert D.T., Smalley R.E., Lou L., Kim S.G. Unraveling nanotubes: Field emission from an atomic wire. Science 1995; 269: 1550-1553.
5. Wang Q.H., Yan M., Chang R.P.H. Flat panel display prototype using gated carbon nanotube field emitters. Appl. Phys. Lett. 2001; 78: 1294-1296.
6. Mauger M., Vu T.V. Vertically aligned carbon nanotube arrays for giant field emission displays. J. Vac. Sci. Technol. B 2006; 24: 997-1003.
7. Reyes-Mena A., Jensen Ch., Bard E., Turner D., Erdmann K.G. Miniature X-ray tubes utilizing carbon-nanotubebased cold cathodes. Advances in X-ray Analysis 2005; 48: 204-209.
8. Matsumoto T., Mimura H. Point X-ray source using graphite nanofibers and its application to X-ray radiography. Appl. Phys. Lett. 2003; 82: 1637-1639.
9. Saito Y., Uemura S., Hamaguchi K. Cathode ray tube lighting elements with carbon nanotube field emitters. Jpn. J. Appl. Phys. 1998; 37: L346-L348.
10. Croci M., Arfaoui I., Stöckli T., Chatelain A., Bonard J.-M. A fully sealed luminescent tube based on carbon nanotube field emission. Microelectron. J. 2004; 35: 329-336.
11. Yasutomo Y., Ohue W., Gotoh Y., Tsuji H. Frequency mixing with a tetrode vacuum transistor. Future of Electron Devices, Kansai, 2012 IEEE International Meeting (IMFDK2012).
12. Sabaut L., Ponard P., Mazellier J.-P., Legagneux P. Electrostatic modeling of an in-plane gated field emission cathode. J. Vac. Sci. Technol. B. 2016; 34: 02G101-7.
13. Yuan X., Zhu W., Zhang Y., Xu N., Yan Y., Wu J., Shen Y., Chen J., She J. A Fully-Sealed Carbon-Nanotube Cold-Cathode Terahertz Gyrotron. Scientific Reports 6. 2016. Article number: 32936.
14. Paoloni C., Carlo A., Brunetti F., Mineo M. Design and Fabrication of a 1 THz Backward Wave

- Amplifier. *Terahertz Science and Technology* 2011; 4: 1102-1110.
15. Rupesinghe N.L., Chhowalla M., Teo K.B.K., Amaratunga G.A.J. Field emission vacuum power switch using vertically aligned carbon nanotubes. *J. Vac. Sci. Technol. B* 2003; 21.1: 1071-1076.
  16. Eletskaa A.V. Carbon nanotube-based electron field emitters. *Phys. Usp.* 2010; 53: 863-892.
  17. Bocharov G.S., Eletskaa A.V. Theory of Carbon Nanotube (CNT)-Based Electron Field Emitters. *Nanomaterials* 2013; 3: 393-442.
  18. Murphy E.L., Good R.H. Thermionic Emission, Field Emission, and the Transition Region. *Phys. Rev.* 1956; 102: 1464-1473.
  19. Mayer A., Lambin Ph. Quantum-mechanical simulations of field emission from carbon nanotubes. *Carbon* 2002; 40: 429-436.
  20. Sun J.P., Zhang Z.X., Hou S.M., Zhang G.M. Work function of single-walled carbon nanotubes determined by field emission microscopy. *Appl. Phys. A* 2002; 75: 479-483.
  21. Vincent P., Purcell S.T., Journe C., Binh V.T. Modelization of resistive heating of carbon nanotubes during field emission. *Phys. Rev. B* 2002; 66: 075406.
  22. Banerjee P.K., Butterfield R. Boundary element methods in engineering science. McGRAW-HILL book company (UK) Limited. London, 1981. 452 p.
  23. Brebbia C.A., Telles J.C.F., Wrobel L.C. Boundary element techniques. Springer-verlag. Berlin, Heidelberg, New York, Tokyo, 1984. 464 p.
  24. Shoup T.E. Applied numerical methods for microcomputers. Prentice-Hall, 1984. 194 p.
  25. Bocharov G.S., Eletskaa A.V. Thermal instability of field emission from carbon nanotubes. *Tech. Phys.* 2007; 52(4): 498-503.
  26. Bocharov G.S., Eletskaa A.V., Sommerer T.J. Optimization of the parameters of a carbon nanotube-based field-emission cathode. *Tech. Phys.* 2011; 56(4): 540-545.
  27. Ziman J.M. Electrons and phonons. The theory of transport phenomena in solids. Oxford at the Clarendon press, 1960. 554 p.
  28. Hone J., Llaguno M.C., Biercuk M.J., Johnson A.T., Batlogg B., Benes Z., Fischer J.E. Thermal properties of carbon nanotubes and nanotube-based materials. *Appl. Phys. A* 2002; 74: 339-343.
  29. Paulini J., Klein T., Simon G. Thermo-field emission and the Nottingham effect. *J. Phys. D: Appl. Phys.* 1993 (Printed in the UK); 26: 1310-1315.
  30. Wei W., Liu Y., Wei Y., Jiang K., Peng L.-M., Fan S. Tip cooling effect and failure mechanism of field-emitting carbon nanotubes. *Nano Lett.* 2007; 7: 64-68.
  31. Huang N.Y., Chen J.C., Chen J., Deng S.Z., Xu N.S., Bishop H., Huq S.E., Wang L., Zhong D.Y., Wang E.G., Chen D.M. Mechanism responsible for initiating carbon nanotube vacuum breakdown. *Phys. Rev. Lett.* 2004; 93: 075501.